A physical explanation of the temperature dependence of physiological processes mediated by cilia and flagella

Stuart Humphries

Supporting Information Appendix

Model Derivations for eukaryotic cilia

My starting point is the force generated by a moving eukaryotic cilium, which is simply the product of cilial length, beat frequency, tip amplitude and the local drag coefficients of the cilial rod as it moves. The drag coefficients will depend on the external fluid viscosity μ_f. The power required to generate this force is given by multiplying the force itself by the product of beat frequency and tip amplitude (essentially the velocity of the cilial tip). To this must be added the power required to overcome the elasticity of the cilial rod, which includes terms for the Young's modulus of the cilium and the wavelength of the wave passing along it (1). Evidence suggests that the stiffness of systems built from molecular motors varies directly with external load (2-4), which will be determined by the external fluid viscosity μ_f.

In contrast to the power required to drive a cilium, the power available will depend on the number of molecular motors involved (likely to be directly proportional to cilial length (5)), the rate of transport of adenosine triphosphate (ATP) to the cilial axoneme, and the rate of hydrolysis of this ATP. Evidence suggests that ATP concentrations in cells are maintained at very high concentrations and thus we can assume simple zeroth-order reaction kinetics, such that ATPase activity is independent of ATP concentration (6), and the latter two processes can be approximated by a diffusion term. This diffusion term will be a positive function of the temperature of the cell (T_c), and an inverse function of the viscosity of the surrounding medium (in this case the cellular contents μ_c) and the size of the diffusing molecule (ATP). Assuming zeroth-order kinetic also means that we implicitly recognise that diffusion and hydrolysis are the limiting step in the energy supply chain. Assuming ATP concentration is at steady state

implies that synthesis and regeneration of ATP are sufficient to maintain the concentration even if their rates vary with temperature.

The power available for ciliary beating can be shown to be dependent on temperature, the length of the cilium, and the concentration of ATP supplying the cilium. It is also dependent on the inverse of the viscosity of the cell and the size of ATP molecules.

Following slender body theory (7), the hydrodynamic force exerted by a single cilium can be approximated as

$$F \sim \left(\xi_{\perp} + \xi_{\parallel}\right) L f a \qquad \text{(S1)}$$

where $\xi_{\perp}$ and $\xi_{/\!/}$ are the local drag coefficients for the effective (perpendicular) and recovery (parallel) strokes, respectively. Here also *L* is the length of the cilium, *f* its beat frequency, and *a* the amplitude of the movement of the cilial tip.

The difference between the two local drag coefficients ($\xi_{\perp}$ and $\xi_{/\!/}$) is the key to efficient beating in the low Reynolds number regime in which cilia operate, with

$$\xi_{\perp} = f_{\perp}\left(\mu_f\right) > \xi_{\parallel} = f_{\parallel}\left(\mu_f\right) \qquad \text{(S2)}$$

where μ_f is the dynamic viscosity of the surrounding fluid. The following reasoning also applies if a more precise calculation of *F* is used such as in appendix I of Guirao and Joanny (8).

With the simplifying assumption of a constant cilial beat pattern, we can treat the sum of local drag coefficients as a function of μ_f, such that the power required to exert the force *F* is

$$P_r \simeq \mu_f L \left(f a\right)^2 + a^2 L Q S K^2 f / \lambda^4 \qquad \text{(S3)}$$

as the *fa* term has the dimensions of velocity [LT^{-1}]. The additive term is that proposed by Machin (1) for the power required to overcome the elasticity of the cilial rod, and includes

terms for the Young's modulus (Q) of the cilium and the wavelength (λ) of the wave passing along it, as well as the cross-sectional area (S) and radius of gyration (K) of the flagellum. Evidence suggests that the stiffness of systems built from molecular motors varies directly with external load (2-4, 9) allowing us to replace Q with viscosity of the external fluid μ_f

$$P_r \simeq \mu_f L(fa)^2 + a^2 L \mu_f f / \lambda^4 \quad \text{(S4)}$$

In contrast to the power required, the power available to a cilium will depend on the number of molecular motors involved (likely to be directly proportional to cilial length (5) L), the rate of transport of ATP to the cilial axoneme, and the rate of hydrolysis of this ATP. If we assume sufficiently high ATP concentrations at a steady state then simple zeroth-order reaction kinetics can be assumed (6) and hydrolysis and transport of ATP can be described by a diffusion term, which can be approximated via Fick's Law:

$$I = 4DsC_\infty \quad \text{(S5)}$$

where I is the adsorption rate, s the adsorber radius, C_∞ the far-field concentration of ATP (assumed to be independent of temperature) and D its diffusion coefficient (10). This approximation describes diffusion across the cross-section of the cilium and does not account for diffusion along its length. Extension of the model using more complex formulations accounting for cilial length (6, 11) would result in the same linear dependence on D but would more accurately portray the length dependence of beat frequency. From the Stokes-Einstein model of diffusion we see that D is a function of temperature, the surrounding medium (in this case the cellular contents), and the size of the diffusing molecule:

$$D = k_B T_c / 6\pi\mu_c r \quad \text{(S6)}$$

Here k_B is the Boltzmann constant, T_c cell temperature in Kelvin, r the radius of the ATP molecule, and μ_c the viscosity of the cell contents.

An estimate of the available power for the cilium can be made by including two final terms: the Avagadro number N_A converting the amount of ATP to a known mass; and a term

representing the efficiency of the dynein molecules in the axoneme *E* (the force generated per unit mass of ATP). For simplicity, I assume *E* is not temperature dependent (although in reality *E* is temperature dependent, the dependence is relatively small over biologically relevant temperature ranges). Hence

$$\begin{aligned} P_a &= 4DsLC_\infty N_A E \\ &= 2k_B T_c sLC_\infty N_A E \Big/ 3\pi\mu_c r \end{aligned} \tag{S7}$$

Equating the available power to that required ($P_a = P_r$), we obtain an expression for the beat frequency of the cilium via

$$\frac{2k_B T_c sLC_\infty N_A E}{3\pi\mu_c r} \simeq \mu_f L(af)^2 + \frac{a^2 L\mu_f f}{\lambda^4} \tag{S8}$$

and after removing (uninteresting) constant terms we obtain

$$\begin{aligned} \frac{C_\infty T_c L}{\mu_c} &\propto \mu_f L(af)^2 + \frac{a^2 L\mu_f f}{\lambda^4} \\ f &\propto \frac{\sqrt{\mu_c\mu_f a^2 + C_\infty T_c \lambda^8}}{a\lambda^4\sqrt{\mu_c\mu_f}} - \frac{1}{\lambda^4} \end{aligned} \tag{S9}$$

indicating that the ciliary beat frequency is a function of temperature, the viscosity of the cell and of the surrounding fluid, the length of the cilium, the wavelength of its beat and its tip amplitude, as well as the concentration of ATP supplying the cilium.

The effect of temperature can be compared to empirical results. The expression for *f* contains several temperature-dependent terms. For the general case where the temperature of the cilium-bearing cell is at thermal equilibrium with its environment ($T_c = T_f$) and assuming that the viscosity of the cell contents scales with temperature in the same way as does the surrounding fluid, we can use an exponential description of viscosity-temperature relationships, $\mu = \left(e^T\right)^x$, where *x* is the slope from an exponential fit to the temperature-viscosity function. This empirical description of a power-law fluid with exponential dependence of viscosity on

temperature (12) has proved difficult to improve on for water due to theorized molecular bonding (13).

On the assumption of a constant concentration of ATP and constant tip amplitude, equation (S9) reduces to

$$f \propto \frac{\sqrt{\left(e^{T_f}\right)^{x+y} a^2 + C_\infty T_f \lambda^8}}{a\lambda^4 \sqrt{\left(e^{T_f}\right)^{x+y}}} - \frac{1}{\lambda^4} \tag{S10}$$

where *x* is the exponent from an exponential fit to the temperature-viscosity function for the fluid and *y* the equivalent term for the cell.

This derivation suggests that in addition to strong temperature dependence, beat frequency *f* is dependent on ATP concentration (C_∞), temperature (*T*), tip amplitude (a) and wavelength (λ), but these effects will remain constant with respect to temperature. Interestingly, cilial length (*L*) drops out. This may not be true for flagella where experimental data suggests length is important (see below).

Holding all non-temperature terms in equation (S9) constant and replacing with aggregated fitting constants ($c_1 ... c_n$)

$$f = \frac{\sqrt{c_1 T + c_2 \left(e^T\right)^{x+y}}}{\sqrt{\left(e^T\right)^{x+y}}} - c_3 = \sqrt{c_2 + c_1 T e^{-T(x+y)}} - c_3 \tag{S11}$$

allows comparison to experimental data for temperature-beat frequency relationships. As both *x* and y are negative, for large values of *T* the exponential term becomes significantly larger than c_2 and equation (S11) can be further simplified to

$$f = \sqrt{c_1 T} e^{\frac{-T(x+y)}{2}} - c_3 \tag{S12}$$

When fluid viscosity (μ_f) is manipulated independently of temperature T_c and μ_c are held constant and the derived dependency of beat frequency (equation S9) reduces to

$$f = \frac{\sqrt{c_1\mu_f + c_2}}{\sqrt{\mu_f}} - c_3 \qquad \text{(S13)}$$

Special cases

Comparison to the Arrhenius equation.

The Arrhenius equation describes the temperature dependence of the reaction rate constant (*k*):

$$k = Ae^{-E_a/RT}, \qquad \text{(S14)}$$

where *A* is a pre-exponential factor, E_a the activation energy of the chemical reaction, and *R* is the gas constant (~8.3 J K^{-1} Mol^{-1}).

Comparison to generic power-law functions.

The general power relationship $f \approx \mu_f^m$ can be given explicitly as $f = a \cdot \mu_f^m + b$, where *a* and *b* are constants. Using equation (S13), the model for viscosity, we can see that this approximates a power function with the explicit exponent *m* = -0.5 of Brokaw (14) when $c_2 \to 1$ and $c_1\mu_f << c_2$ (more exactly $c_1 \to 0$) are satisfied.

Derivations for eukaryotic flagella

Rikmenspoel (15) cites Taylor (16) for the hydrodynamic work done by the flagellum of spermatozoa with a planar beat:

$$W = \frac{4\pi^3 \mu L f^2 a^2}{0.62 - \ln\left(2\pi\rho/\lambda\right)} \quad \text{(S16)}$$

where *L* is flagella length, *a* wave is amplitude, ƒ is the beat frequency (directly replaceable by angular frequency ω for helical waveforms), λ is wavelength and ρ is the radius of the cross-section of the flagellum. The results are given in erg s^{-1}, suggesting that this is actually power (J s^{-1}).

As for the cilial derivation, an additive term accounting for internal elasticity is needed, giving the total power required as

$$P_r \simeq \mu_f L(fa)^2 + a^2 LQf/\lambda^4 \quad \text{(S17)}$$

Which is identical to equation (S4) when we assume that $Q \propto \mu_f$ as before. With power available (P_a) derived as for cilia, the final expressions for the two are identical.

Derivations for Bacterial and Archaeal flagella

Archaeal and bacterial flagella rely on essentially the same hydrodynamic principles as eukaryotic flagella for the generation of motile force (7, 17, 18), however, the mechanism of generating this movement differs. In terms of required power, the equation for eukaryotes (S4) needs to be modified such that the elasticity term is replace with the power required to rotate the body of the organism. Locomotion using a rotating helix requires a body (17) and so the energetic costs of the rotary flagellum include those associated with the torque for the cell body, τ. In this case we can use the expression for torque for a rotating sphere about a central axis at low Reynolds number (19):

$$\tau = -8\pi\mu_f b^3 \omega \quad \text{(S18)}$$

where *b* is the radius of the sphere and ω the angular velocity (a vector quantity). The magnitude of the angular velocity of the cell is it's rotational speed (rotational frequency) and is

assumed to be linearly related to the rotational speed of the helical flagellum (17). The two terms are thus used interchangeably here. The product of the torque and angular velocity gives the power required for that torque, such that

$$P_r \simeq \mu_f L(\omega a)^2 + 8\pi\mu_f b^3\omega^2 \quad \text{(S19)}$$

Instead of linearly moving dynein, Archaeal and Bacterial flagella are driven by a rotational molecular motor (20). For Archaea ATP is the energy source (20). The mechanical difference from Eukaryotic flagella suggests that the expression for available power (equation S7) for Archaea should be modified to

$$\begin{aligned} P_a &= 4Dsr_{rot}C_\infty N_A E \\ &= 2k_B T_c s r_{rot} C_\infty N_A E / 3\pi\mu_c r \end{aligned} \quad \text{(S20)}$$

where r_{rot}, the radius of the rotary mechanism, replaces the length of the flagellum, L. The result is that for Archaea the predicted relationships with temperature are modified by the additional dependence of P_r on angular velocity, ω. The resulting temperature and viscosity functions are

$$\omega \propto \sqrt{c_7 T_c}\, e^{\frac{-T(x+y)}{2}} + c_8 \quad \text{(S21)}$$

which is functionally identical to S12, and

$$\omega \propto \frac{c_9}{\sqrt{\mu_f + c_{10}}} \quad \text{(S22)}$$

which differs only slightly from S13.

In Bacteria energy delivery is via proton (H^+) or sodium ion (Na^+) motors (flow of ions down an electrochemical gradient across the cytoplasmic membrane into cell (18, 21)). In this case we can consider r as the radius of the protons or sodium ions involved in the transfer process and D their diffusivity. As ions are charged the flux, J (rate per unit area) across the cell

membrane is driven by both diffusion (via the H^+ or Na^+ concentration gradient ∇C) and an electric field ($\nabla\phi$), and can be described by the Nernst-Planck equation. Here Fick's law is used to describe the effect of the concentration gradient

$$J = -D\nabla C\,, \tag{S23}$$

while Planck's equation describes the ion-flux due to an electrical field:

$$J = -m\frac{z}{|z|}C\nabla\phi \tag{S24}$$

where *z* is the valence (the number of covalent bonds possible) of the ionic species and *m* the mobility of the ions. Fick's law and Planck's equation are related via the Nernst-Einstein relationship

$$m = D\frac{|z|F}{RT} \tag{S25}$$

Here *F* is the Faraday constant. Combining S23 and S24 gives the Nernst-Planck equation

$$J = -D\left(\nabla C + \frac{zF}{RT}C\nabla\phi\right) \tag{S26}$$

If we divide this equation by the area of the bacterial rotor we obtain a function describing the rate at which ions are transported across the motor.

$$I = \frac{J}{\pi s^2} = \frac{D\nabla C - \frac{DzF}{RT}C\nabla\phi}{\pi s^2} \tag{S27}$$

This further reduces to a single term for temperature when equation S6 is substituted for *D* in the same way as for equations S5 and S6:

$$I = \frac{\nabla Ck\left(RT - F\nabla\phi z\right)}{6\pi^2\mu_c r s^2 R} \tag{S28}$$

These modifications lead to an expression for bacteria that is equivalent to equation (S9):

$$\frac{4r_{rot}}{\pi}\left(\frac{T\nabla C}{6\pi\mu_c}-\frac{CF\nabla\phi z}{6\pi\mu_f R}\right)\propto\mu_f L\left(a\omega\right)^2_{\max}+8\pi\mu_f b^3\omega^2$$

$$\omega\propto\frac{\sqrt{6L}\sqrt{RT\nabla C-CF\nabla\phi z}}{3\pi\sqrt{R\mu_c\mu_f La^2+b^3}} \qquad \text{(S29)}$$

And so to a form equivalent to equations (S12) and (S21)

$$\omega\propto\sqrt{c_7T_c-c_8}e^{\frac{-T(x+y)}{2}}+c_9 \qquad \text{(S30)}$$

differing only in that temperature (T_c) is modified by subtraction of a constant, while the equivalent to S13 is identical to that for Archaea (S22).

References:

1. Machin KE (1958) Wave propogation along flagella. *J Exp Biol* 35:796–806.

2. Gao Y (2006) A Simple Theoretical Model Explains Dynein's Response to Load. *Biophys J* 90:811–821.

3. Cross RA (2004) Molecular motors: Dynein's gearbox. *Curr Biol* 14:R355–6.

4. Sznitman J, Purohit PK, Lamitina T, Arratia PE (2010) Material properties of *Caenorhabdites elegans* swimming at low Reynolds number. *Biophys J* 98:617–626.

5. Alexander RM (1971) *Size and shape* (Hodder Arnold).

6. Nevo AC, Rikmenspoel R (1970) Diffusion of ATP in sperm flagella. *J Theor Biol* 26:11–18.

7. Brennen C, Winet H (1977) Fluid mechanics of propulsion by cilia and flagella. *Ann Rev Fluid Mech* 9:339–398.

8. Guirao B, Joanny J (2007) Spontaneous creation of macroscopic flow and metachronal waves in an array of cilia. *Biophys J* 92:1900–1917.

9. Okuno M, Asai DJ, Ogawa K, Brokaw CJ (1981) Effects of antibodies against dynein and tubulin on the stiffness of flagellar axonemes. *J Cell Biol* 91:689–694.

10. Berg HC (1983) *Random walks in biology*. Princeton. 152pp.

11. Adam DE, Wei J (1975) Mass transport of ATP within the motile sperm. *J Theor Biol* 49:125–145.

12. Reynolds O (1886) On the Theory of Lubrication and Its Application to Mr. Beauchamp Tower's Experiments, Including an Experimental Determination of the Viscosity of Olive Oil. *Proceedings of the Royal Society of London* 40:191–203.

13. Seeton CJ (2006) Viscosity–temperature correlation for liquids. *Tribol Lett* 22:67–78.

14. Brokaw CJ (1966) Effects of increased viscosity on the movement of some invertebrate spermatozoa. *J Exp Biol* 45:113–139.

15. Rikmenspoel R, Sinton S, Janick JJ (1969) Energy conversion in bull sperm flagella. *J Gen Physiol* 54:782–805.

16. Taylor G (1952) The Action of Waving Cylindrical Tails in Propelling Microscopic Organisms. *Proc Roy Soc Lond A* 211:225–239.

17. Lauga E, Powers TR (2009) The hydrodynamics of swimming microorganisms. *Rep Prog*

Phys 72:096601.

18. Xing J, Bai F, Berry RM, Oster G (2006) Torque-speed relationship of the bacterial flagellar motor. *Proc Nat Acad Sci* 103:1260–1265.

19. Happel J, Brenner H (1983) *Low Reynolds number hydrodynamics* (Kluwer, The Hague). 553pp.

20. Bardy SL, Ng SYM, Jarrell KF (2003) Prokaryotic motility structures. *Microbiology* 149:295–304.

21. Berg HC (2000) Motile behavior of bacteria. *Phys Today* 53:24–30.

Supplementary Figures S1-S10

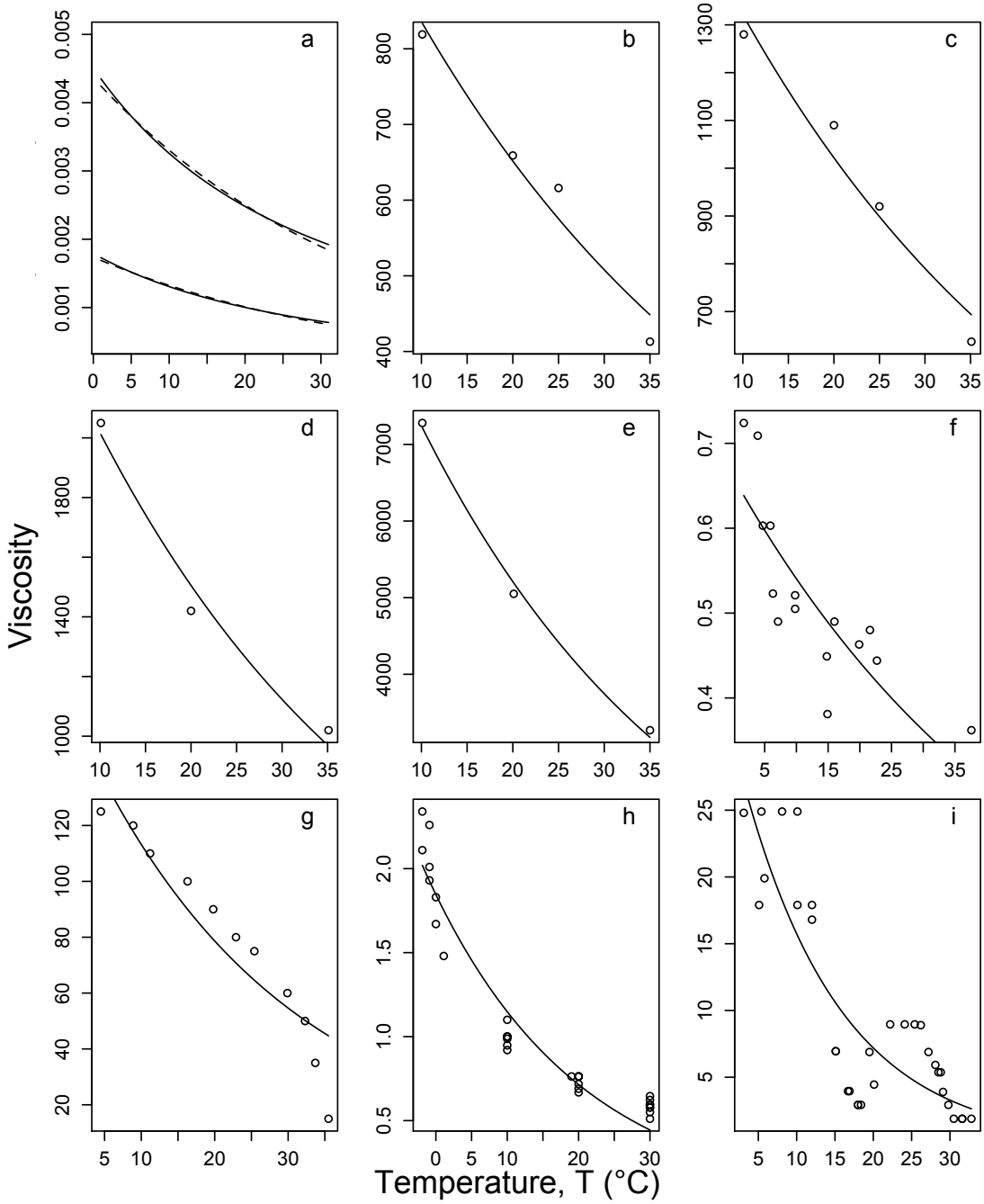

Fig. S1 Cellular rheology. (a) Relationship between temperature and dynamic viscosity of pure water (lower solid line) and 35‰ seawater (upper solid line). Broken lines show an exponential description of viscosity-temperature relationships, $\mu = (e^T)^x$. (b-i) The relationship between temperature and an arbitrary viscosity proxy for a selection of cell types. Citations for datasets are given in Supplementary Table S3.

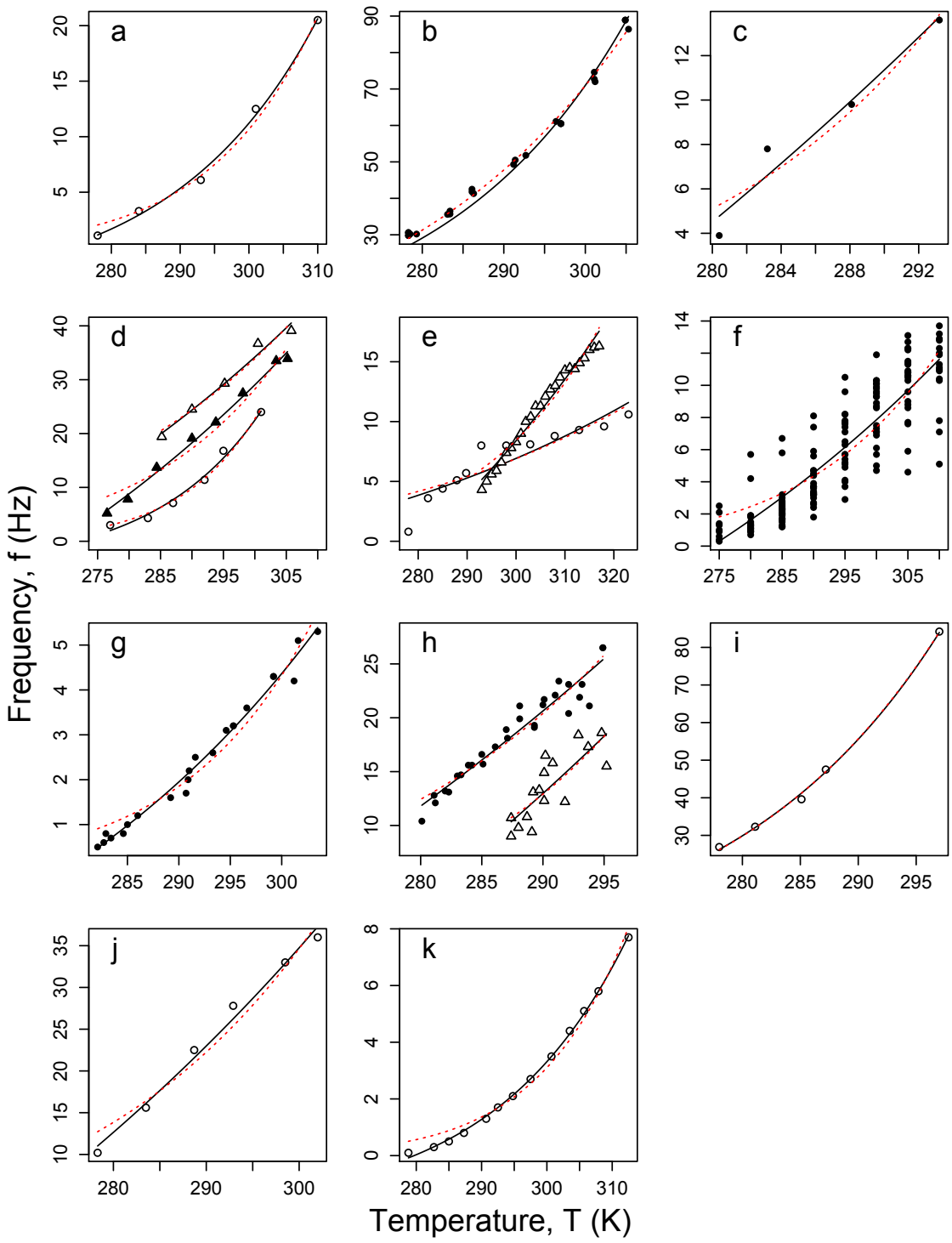

Fig. S2 Eukaryote temperature-frequency relationships. Solid lines are fits for the new model, dashed (red) for the Arrhenius equation. Open symbols indicate data from individual cells, filled symbols data from experimental means. Citations for datasets (panels a - k) are given in Supplementary Table S4.

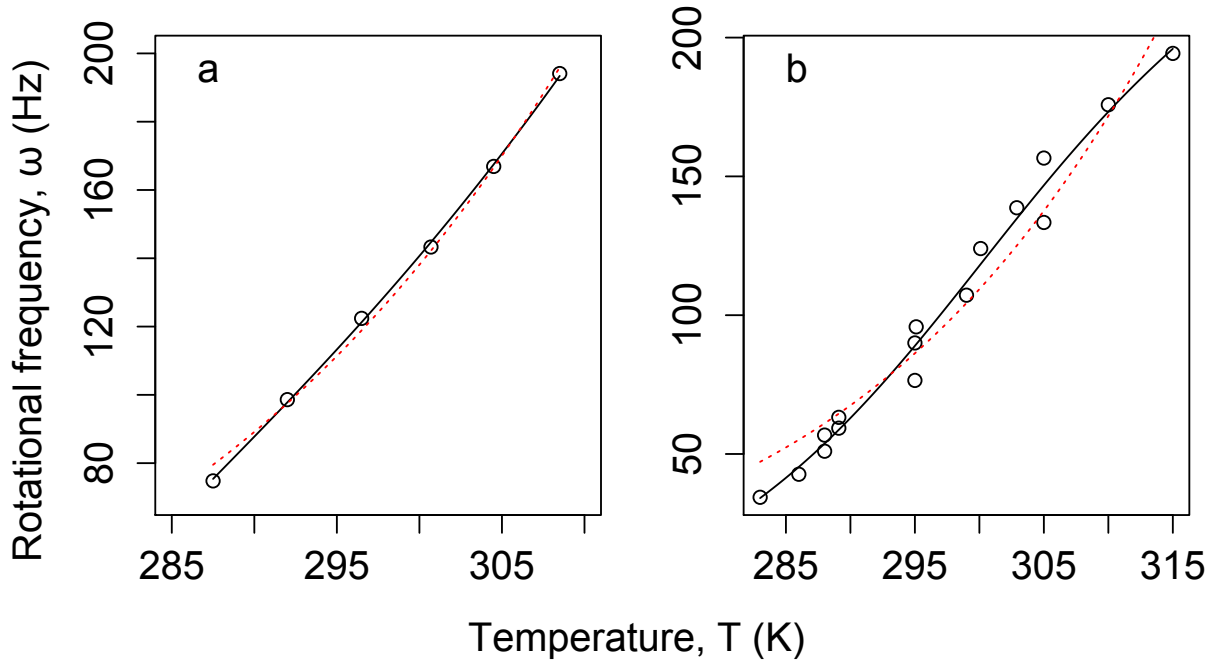

Fig. S3 Prokaryote temperature-frequency relationships. Solid lines are fits for the new model, dashed (red) for the Arrhenius equation. Open symbols indicate data from individual cells, filled symbols data from experimental means. Citations for datasets (panels a and b) are given in Supplementary Table S5.

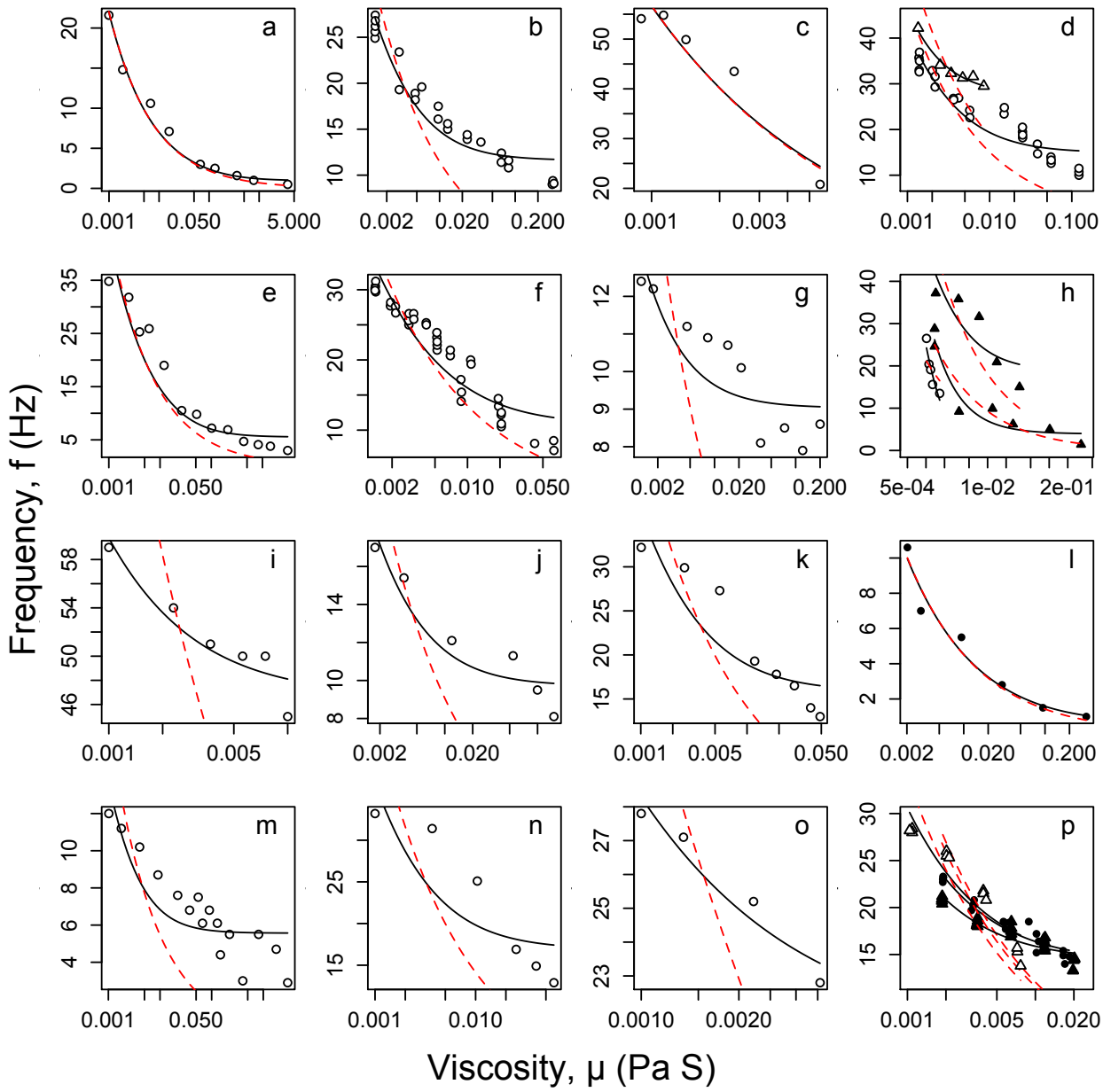

Fig. S4 Eukaryote viscosity-frequency relationships. Solid lines are fits for the new model, dashed (red) for a function based on scaling as $\mu_f^{-0.5}$. Open symbols indicate data from individual cells, filled symbols data from experimental means. Citations for datasets (panels a - p) are given in Supplementary Table S6.

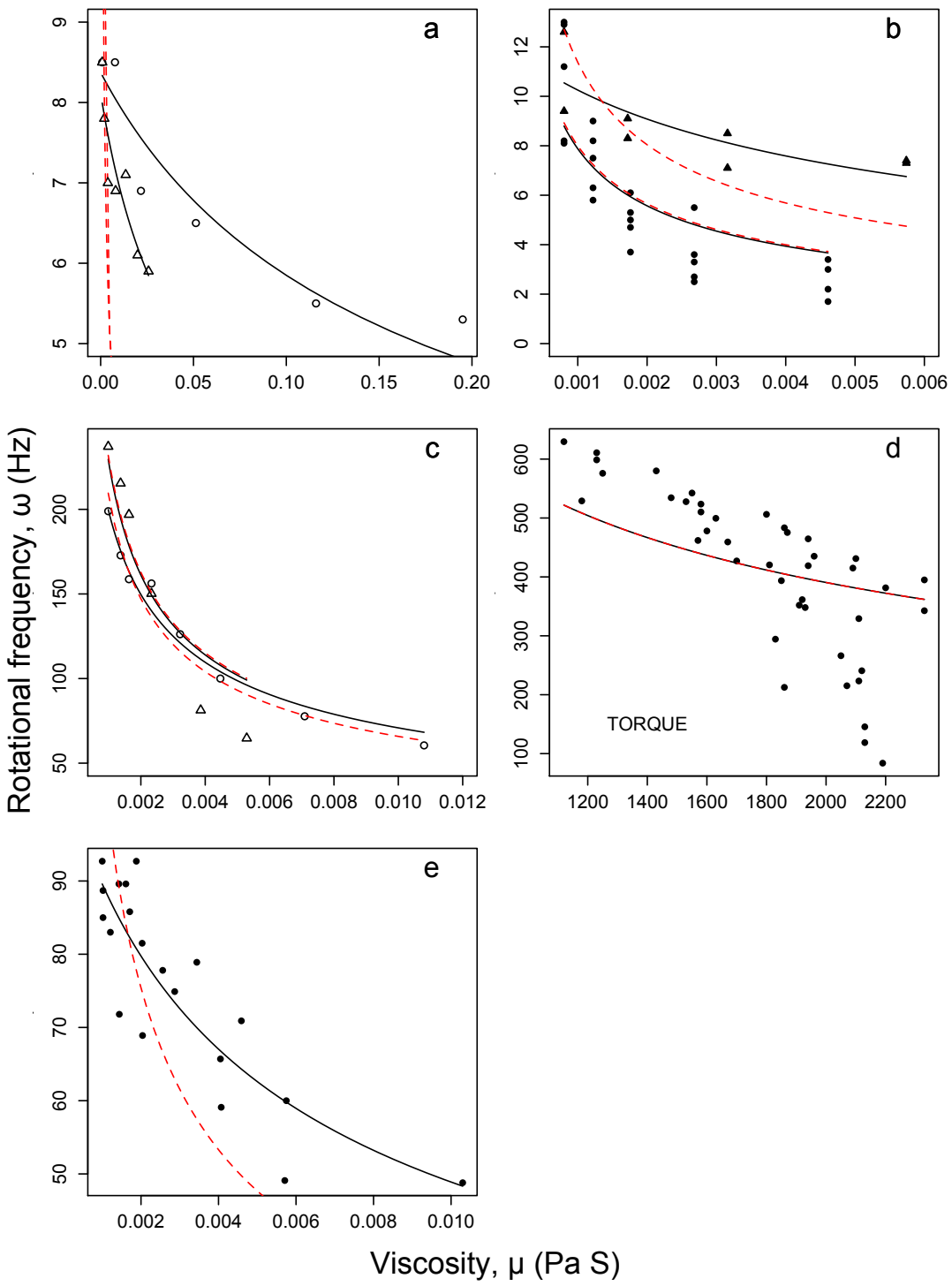

Fig. S5 Prokaryote viscosity-frequency relationships. Solid lines are fits for the new model, dashed (red) for a function based on scaling as $\mu_f^{-0.5}$. Note panel d uses data on Torque as a proxy for viscosity. Open symbols indicate data from individual cells, filled symbols data from experimental means. Citations for datasets (panels a - e) are given in Supplementary Table S7.

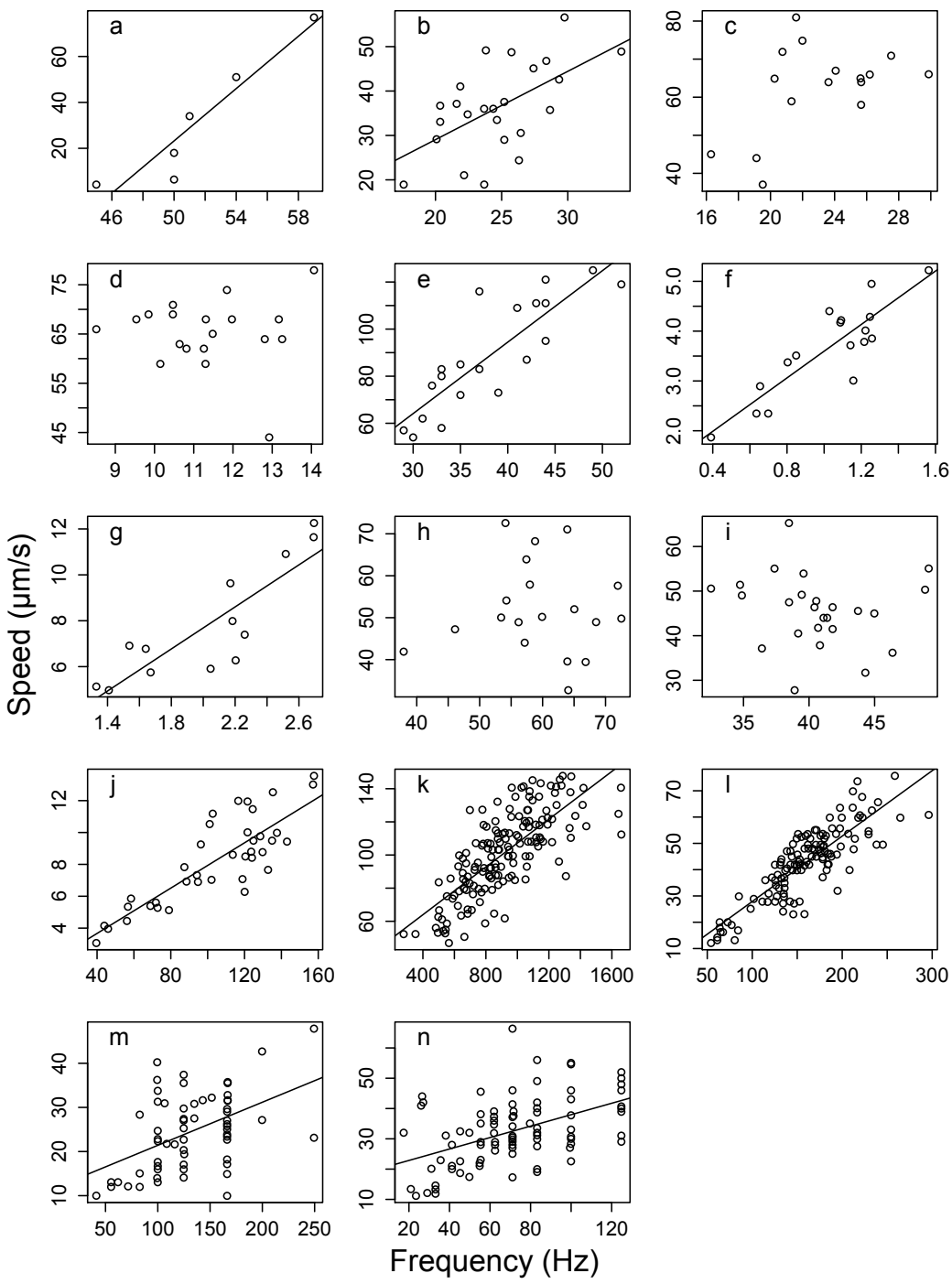

Fig. S6 Relationships between beat and rotational frequencies and swimming speeds of unicells. Solid lines are significant linear fits, with effects sizes (*r*) given in figure 3. Four of 14 datasets did not show a significant linear relationship, but all confidence intervals for the effect size include a positive relationship. Citations for datasets (panels a - n) are given in Supplementary Table S2.

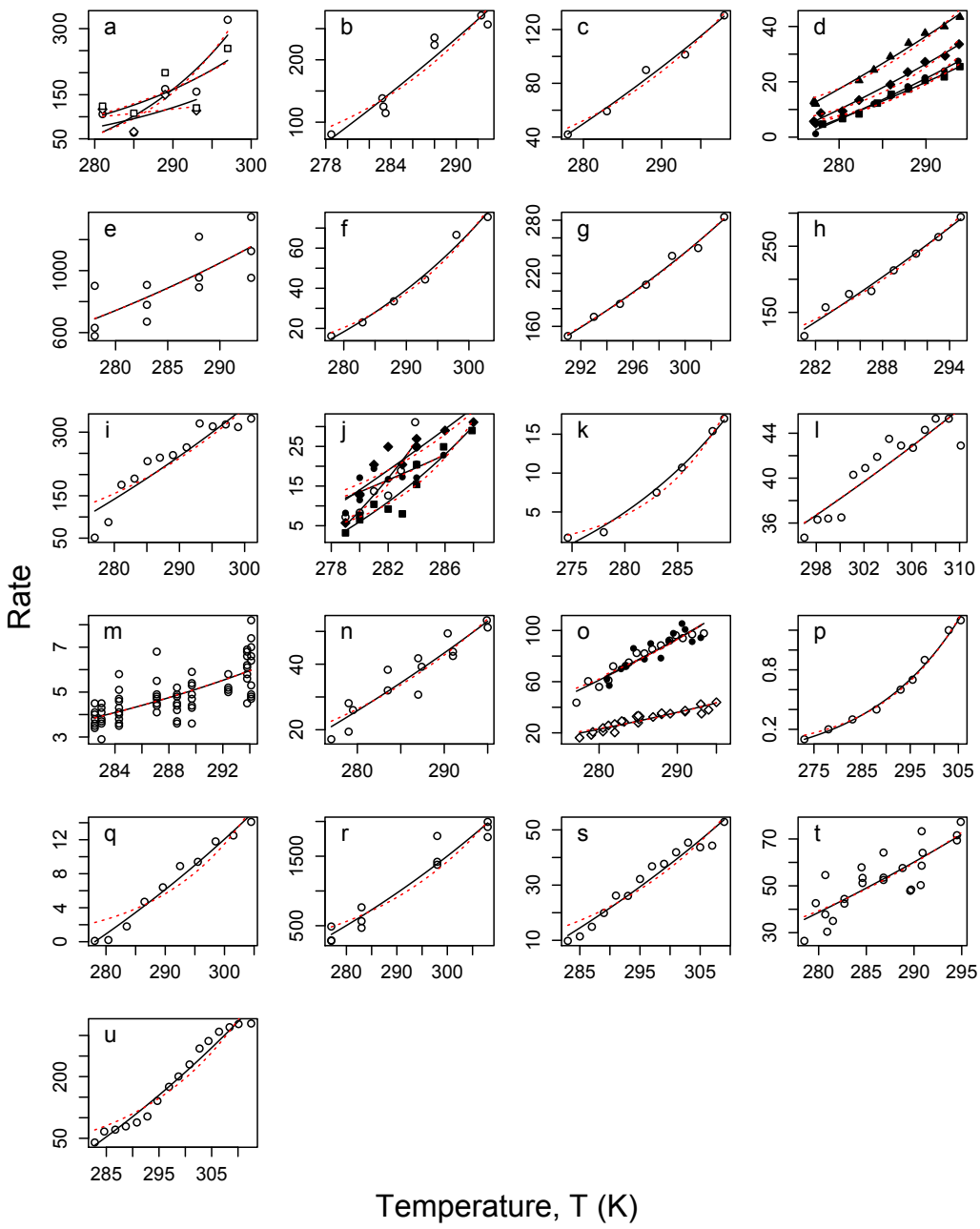

Fig. S7 Eukaryote temperature-rate relationships. Rates for panels a-c, e-i, l, m, r, s and u are swimming speeds (µm/s), while for panels d, j, k, n-p and t they are pumping rates (volume/time/individual or volume/time/unit mass). The rate in panel o (open diamonds, Gray 1923) is speed of travel of a tracer due to cilial transport (mm/s) and in panel q it is the rate of doing work (pumping, erg/s). Solid lines are fits for the new model, dashed (red) for the Arrhenius equation. Open symbols indicate data from individual cells, filled symbols data from experimental means. Citations for datasets (panels a - u) are given in Supplementary Table S8.

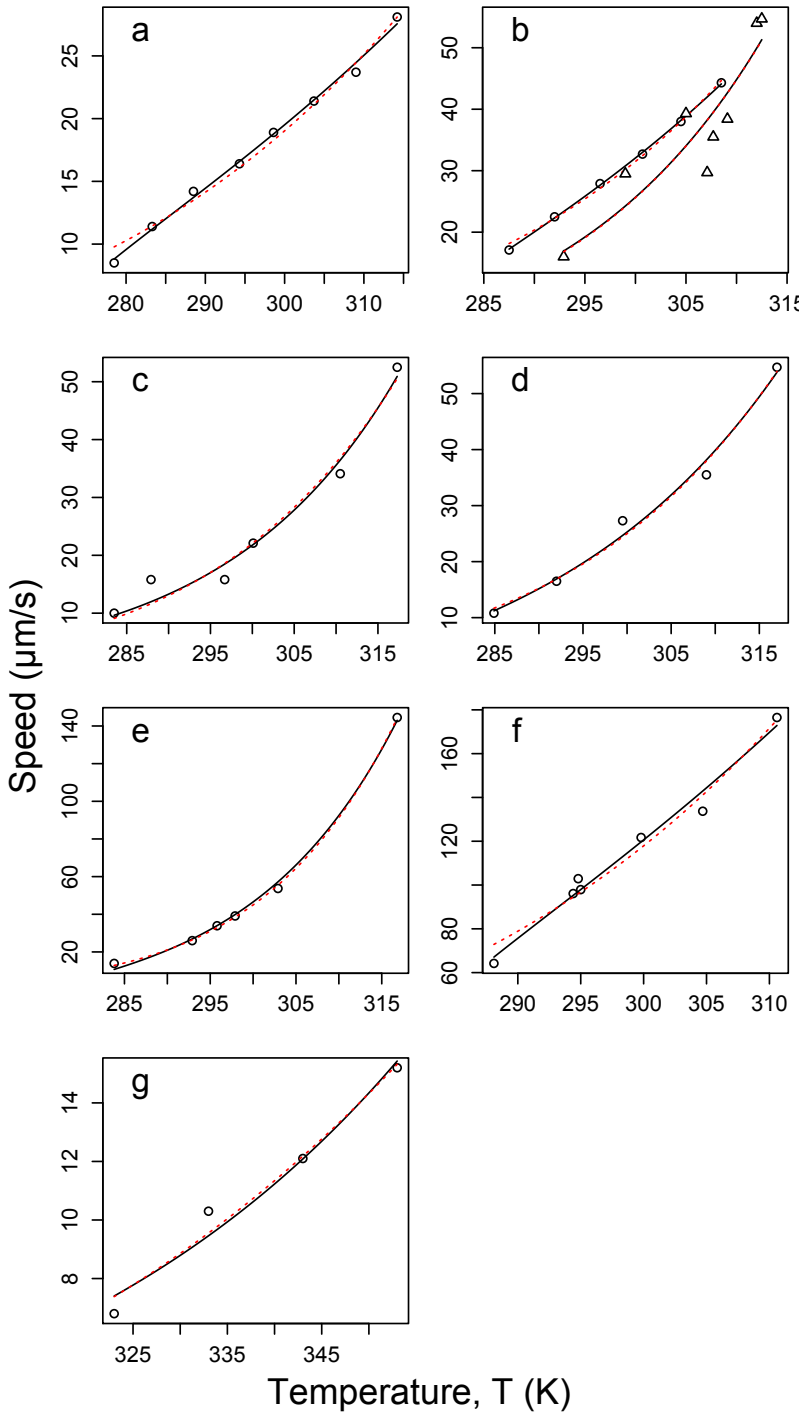

Fig. S8 Prokaryote temperature-speed relationships. Solid lines are fits for the new model, dashed (red) for the Arrhenius equation. Open symbols indicate data from individual cells, filled symbols data from experimental means. Citations for datasets (panels a - g) are given in Supplementary Table S9.

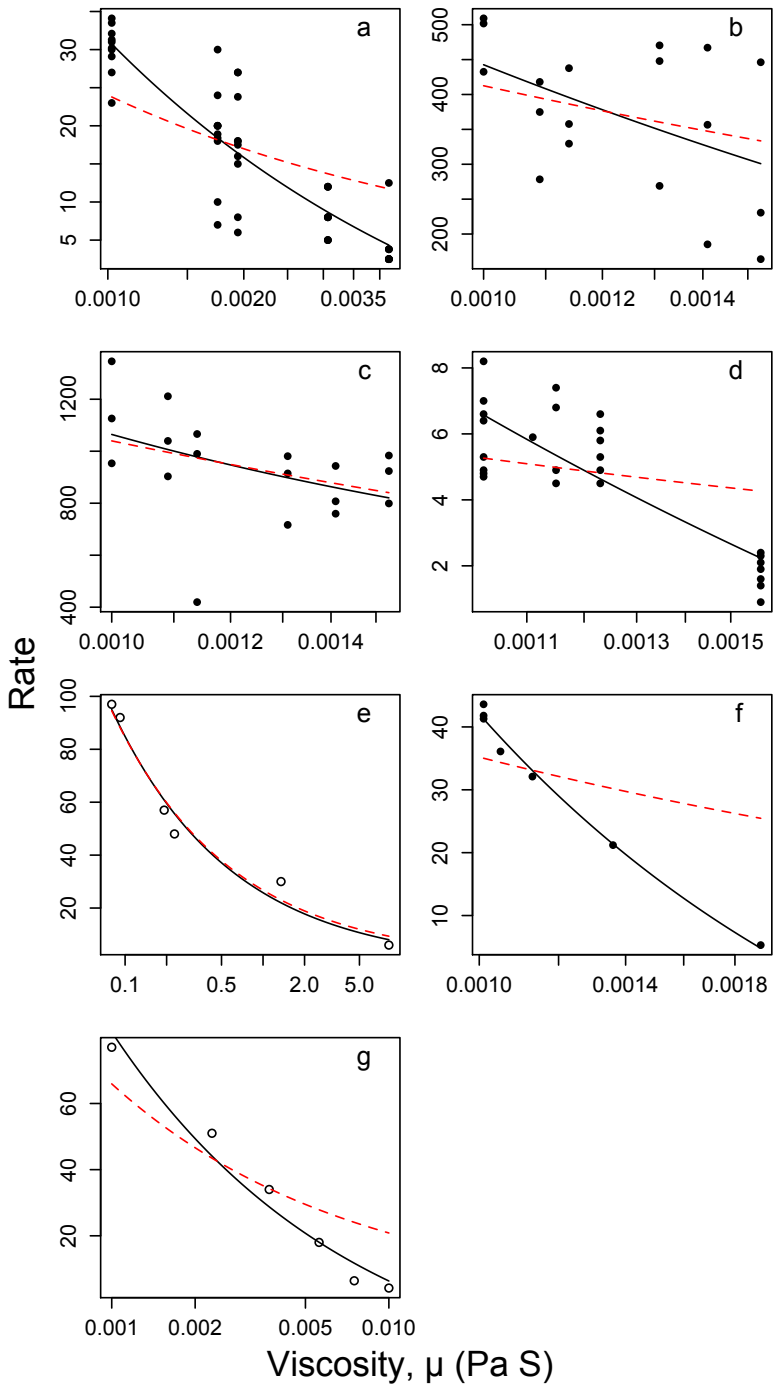

Fig. S9 Eukaryote viscosity-rate relationships. Rates for panels a-e, and g are swimming speeds (μm/s), while for panel f it is pumping rate (volume/time/individual). Solid lines are fits for the new model, dashed (red) for a function based on scaling as $\mu_f^{-0.5}$. Open symbols indicate data from individual cells, filled symbols data from experimental means. Citations for datasets (panels a - g) are given in Supplementary Table S10.

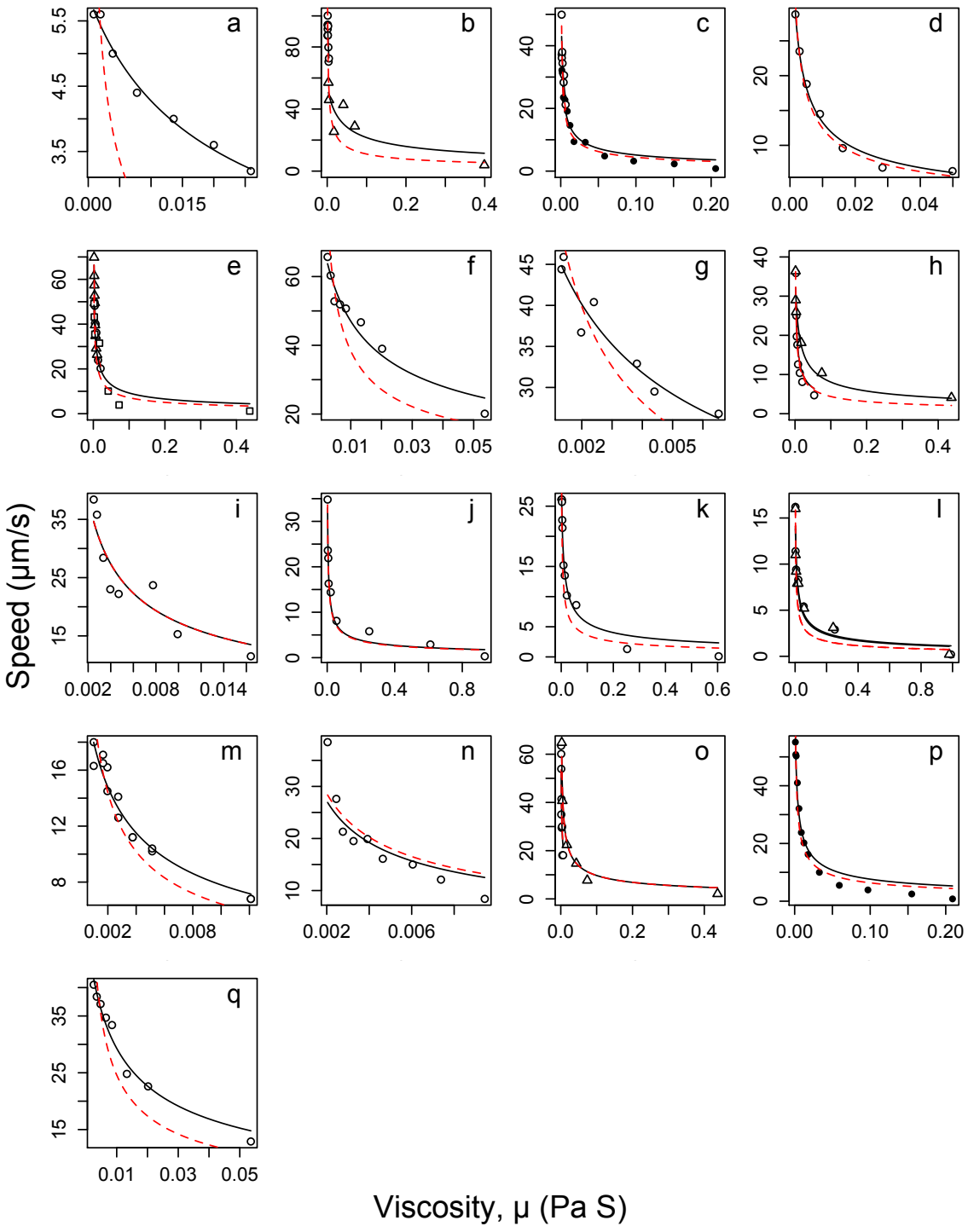

Fig. S10 Prokaryote viscosity-speed relationships. Solid lines are fits for the new model, dashed (red) for a function based on scaling as $\mu_f^{-0.5}$. Open symbols indicate data from individual cells, filled symbols data from experimental means. Citations for datasets (panels a - q) are given in Supplementary Table S11.

Supplementary Tables S1-S10

Table S1. Datasets used for figure 1a.

Section	Sources
Phylogenetic tree (centre)	iTOL Interactive Tree of Life (http://itol.embl.de)
Archaea (green outer sections)	Desmond, E., Brochier-Armanet, C. & Gribaldo, S. (2007) Phylogenomics of the archaeal flagellum: rare horizontal gene transfer in a unique motility structure. *BMC Evol Biol* **7,** 106.
Eukaryotes (pink outer sections)	Brennen, C. & Winet, H. (1977) Fluid mechanics of propulsion by cilia and flagella. *Ann Rev Fluid Mech* **9,** 339–398. Liu, Y. J., Hodson, M. C. & Hall, B. D. (2006) Loss of the flagellum happened only once in the fungal lineage: phylogenetic structure of kingdom Fungi inferred from RNA polymerase II subunit genes. *BMC Evol Biol* **6,** 74. Margulis, L., Corliss, J.O., Melkonian, M. & Chapman, D.J. (eds.) (1991) *Handbook of Protictista*. Jones and Bartlett, Boston. Silflow, C. D. & Lefebvre, P. A. (2001) Assembly and Motility of Eukaryotic Cilia and Flagella. Lessons from *Chlamydomonas reinhardtii*. *Plant Physiol* **127,** 1500–1507.
Bacteria (purple outer sections)	Brennen, C. & Winet, H. (1977) Fluid mechanics of propulsion by cilia and flagella. *Ann Rev Fluid Mech* **9,** 339–398. Garrity, G. *et al.* (2012) *Bergey's Manual of Systematic Bacteriology*. **Vol 1-5,** Springer, New York. Higgins, M. L., Lechevalier, M. P. & Lechevalier, H. A. (1967) Flagellated actinomycetes. *J Bacteriol* **93,** 1446–1451. Leifson, E. (1960) *Atlas of bacterial flagellation.* New York & London, Academic Press. Thormann, K. M. & Paulick, A. (2010) Tuning the flagellar motor. *Microbiology* **156,** 1275–1283.

Table S2. Datasets used for Frequency-Speed analysis (Figs. 3 and S6)

Taxon	n	Source
Escherichia coli	85	Darnton, N. C., Turner, L., Rojevsky, S. & Berg, H. C. (2007) *J Bacteriol* 189, 1756–1764.
Escherichia coli (high viscosity)	61	
Salmonella typhimurium	125	Magariyama, Y. *et al.* (1995) *Biophys J* 69, 2154–2162.
Vibrio alginolyticus	159	
Bos taurus (sperm)	38	Rikmenspoel, R., van Herpen, G. & Eijkhout, P. (1960) *Phys Med Biol* 5, 167–181.
Crithidia deani	25	Gadelha, C., Wickstead, B. & Gull, K. (2007) *Cell Motil Cytoskeleton* 64, 629–643.
Crithidia fasciculata	19	
Crithidia oncopelti	4	Holwill, M. E. J. (1965) *J Exp Biol* 42, 125–137.
Echinus esculentus (sperm)	13	Woolley, D. M. & Vernon, G. (2001) *J Exp Biol* 204, 1333–1345.
Echinus esculentus (sperm, high viscosity)	17	
Ectocarpus silicuosus (gamete)	20	Geller, A. & Müller, D. G. (1981) *J Exp Biol* 92, 53.
Homo sapiens (sperm)	19	Smith, D. J., Gaffney, E. A., Gadêlha, H., Kapur, N. & Kirkman-Brown, J. C. (2009) *Cell Motil Cytoskeleton* 66, 220–236.
Homo sapiens (sperm, high viscosity)	16	
Leishmania major	24	Gadelha, C., Wickstead, B. & Gull, K. (2007) *Cell Motil Cytoskeleton* 64, 629–643.
Ochromonas danica	6	Holwill, M. E. J. & Peters, P. D. (1974) *J Cell Biol* 62, 322–328.

Table S3. Datasets used for cell viscosity-temperature relationships (Fig. S1)

Cell type	Methodology	Exponent estimate	Source
Rat muscle	Tension analysis	-0.0249	Mutungi, G. & Ranatunga, K.W. (1998) J. Physiol., 508(1): 253–265.
		-0.0257	
		-0.0293	
		-0.0330	
Cat nerve	Electron spin resonance	-0.0200	Haak, R.A., Kleinhans, F.W. & Ochs, S. (1976) J. Physiol., 263: 115–137.
Amoeba	Centrifugation	-0.0364	Thornton, F. (1932) Physiol. Zool., 5:246–253.
		-0.0783	Heilbrunn, L. (1929) Protoplas. 8: 58–64.
Nereis egg		-0.0475	Pantin, C. (1924) J. Mar. Biol. Assoc. UK, 13: 331–339.

Table S4. Datasets used for Eukaryote Frequency-Temperature analysis (Fig. S2)

Panel	Species (tissue)	ΔAIC	n	Source
a	*Bos taurus* (sperm flagella)	2.5	5	Rikmenspoel, R. (1984) J. Exp. Biol., 108: 205–230.
b	*Chlamdymonas reinhardii* (flagella)	-20.6	25	Holwill, M. & Silvester, N. (1967) J. Exp. Biol., 47: 249–265.
c	*Ciona intestinalis* (branchial basket cilia)	-0.1	4	Petersen, J.K., et al. (1999) Mar. Biol., 133: 185–192.
d	*Crithidia (Strigomonas) oncopelti* (flagella)	-1.5	6	Holwill, M. & Silvester, N. (1965) J. Exp. Biol., 42: 537–544.
	Crithidia oncopelti (flagella)	-0.2	5	Holwill, M. & McGregor, J.L. (1974) J. Exp. Biol., 60: 437–444.
	Crithidia oncopelti (flagella)	12.3	8	Coakley, C.J. & Holwill, M. (1974) J. Exp. Biol., 60: 605–629.
e	*Homo sapiens* (nasal epithelial cilia)	18.3	25	Jorissen, M. & Bessems, A. (1995) Eur. Arch. Otorhinolaryngol., 252:451–454.
	Homo sapiens (nasal & tracheal epithelial cilia)	-0.8	12	Clary-Meinesz, C., et al. (1992) Biol. Cell., 76: 335–338.
f	*Homo sapiens* (nasal epithelial cilia)	14.2	155	Smith, C. M. *et al*. (2011) *Chest* 140, 186–190.
g	*Lytechinus pictus* (sperm flagella)	19.1	22	Holwill, M. (1969) J. Exp. Biol., 50: 203–222.
h*	*Mytilus edulis* (gill cilia)	2.5	29	Riisgård, H.U. & Larsen, P.S. (2007) Mar. Ecol. Prog. Ser., 343: 141–150.
	Mytilus edulis (gill cilia)	-0.9	16	Stefano, G., et al. (1977) Biol. Bull., 153:618–629.

i	*Oncorhynchus mykiss* (sperm flagella)	-2.0	5	Billard R. & Cosson M.P. (1988) *cited in* Alavi, S.M.H. & Cosson, (2005) Cell. Biol. Int. 29: 101–110.
j	*Stentor polymorphus* (peristomal cilia)	4.9	6	Sleigh, M. (1956) J. Exp. Biol., 33: 15–28.
k	*Taricha granulose* (isolated lung cilia)	31.0	13	Hard, R. & Cypher, C. (1992) Cell Motil. Cytoskeleton, 21: 187–198.

AIC difference calculated as $\Delta AIC = AIC_{Arrhenius} - AIC_{model}$, such that that support for the Arrhenius model gives a negative value. Panel letters refer to figure S2, starred panel letters indicate dataset is used in figure 2d.

Table S5. Datasets used for Prokaryote Frequency-Temperature analysis (Fig. S3)

Panel	Species	ΔAIC	n	Source
a*	*Escherichia coli*	8.5	6	Iwazawa, J., Imae, Y. & Kobayasi, S. (1993) *Biophys J* 64, 925–933.
b	*Streptococcus*	13.7	16	Lowe, G. & Meister, M. (1987) *Nature* 325, 637–640.

AIC difference calculated as $\Delta AIC = AIC_{Arrhenius} - AIC_{model}$, such that support for the Arrhenius model gives a negative value. Panel letters refer to figure S3, starred panel letters indicate dataset is used in figure 2b.

Table S6. Datasets used for Eukaryote Frequency-Viscosity analysis (Fig. S4)

Panel	Species (tissue)	Medium	ΔAIC	n	Source
a	*Bos Taurus* (sperm flagella)	CMC	-3.4	9	Rikmenspoel, R. (1984) *J Exp Biol* 108, 205–230.
b	*Chaetopterus variopedatus* (sperm flagella)	MC	55.1	24	Brokaw, C. (1966) *J Exp Biol* 45, 113–139.
c	*Chlamydomonas* 137c [wild type] (flagella)	Ficoll	-4.0	5	Minoura, I. & Kamiya, R. (1995) *Cell Motil Cytoskel* 31, 130–139.
d	*Ciona intestinalis* (sperm flagella)	MC	42.0	27	Brokaw, C. (1966) *J Exp Biol* 45, 113–139.
		MC	22.2	6	Brokaw, C. (1996) *Cell Motil Cytoskel* 33, 6–21.
e	*Crithidia oncopelti* (flagella)	Unknown	0.2	13	Sugrue, P., Hirons, M., Adam, J. & Holwill, M. (1988) *Biol Cell* 63, 127–131.
f	*Lytechinus pictus* (sperm flagella)	MC	19.9	37	Brokaw, C. (1966) *J Exp Biol* 45, 113–139.
g	*Mesocricetus auratus* (oviductal cilia)	Dextran	31.2	10	Andrade, Y.N. (2005) *J Cell Biol* 168, 869–874.
h*	*Mytilus edulis* (gill cilia)	Dextran*	6.9	5	Riisgård, H.U. & Larsen, P.S. (2007) *Mar Ecol Prog Ser* 343, 141–150.
		PVP	2.3	5	
		Ficoll*	-1.1	7	Rikmenspoel, R. (1976) *Biophys J* 16, 445–470.
		CMC	0.6	5	Yoneda, M. (1962) *J Exp Biol* 39, 307 *cited in* Rikmenspoel, R. (1976) *Biophys J* 16, 445–470.

i	*Ochromonas danica* (hispid flagella)	MC	24.2	6	Holwill, M.E. & Peters, P.D. (1974) *J Cell Biol* 62, 322–328.
j	*Oryctolagus cuniculus* [New Zealand white] (respiratory cilia)	Dextran	14.8	6	Johnson, N., Villalon, M., Royce, F., Hard, R. & Verdugo, P. (1991) *Am Rev Respir Dis* 144, 1091–1094.
k	*Paramecium multimicronucleatum* (cilia)	MC	9.1	8	Machmer, H. (1972) *J Exp Biol* 57, 239–259.
l	*Phragmatopoma* sp. (gill cilia)	Ficoll	-3.8	6	Rikmenspoel, R. (1976) *Biophys J* 16, 445–470.
m	*Rana ridibunda* (oesophageal cilia)	Dextran, PVP, CMC	28.1	16	Gheber, L.A., Korngreen, A. & Priel, Z. (1998) *Cell Motil Cytoskel* 39, 9–20.
n	*Rattus norvegicus* [Wistar] (brain ependymal cilia)	Dextran	4.25	6	O'Callaghan, C., Sikand, K., Rutman, A. & Hirst, R. (2008) *Neurosci Lett* 439, 56–60.
o	*Stentor polymorphus* (peristomal cilia)	MC	12.2	4	Sleigh, M. (1956) *J Exp Biol* 33, 15–28.
p	*Strongylocentrotus pupuratus* (sperm flagella)	MC	62.4	20	Brokaw, C. & Simonick, T. (1977) *J Cell Sci* 23, 227–241.
		MC	76.7	24	
		Ficoll	9.9	12	Pate, E. & Brokaw, C. (1980) *J Exp Biol* 88, 395–397.

AIC difference calculated as $\Delta AIC = AIC_{power} - AIC_{model}$, such that that support for the power model gives a negative value. Media used to adjust viscosity: Dextran; Ficoll; Polyvinyl pyrrolidone (PVP); Methylcellulose (MC); Carboxymethylcellulose (CMC). Panel letters refer to figure S4, starred panel letters (and medium) indicate dataset is used in figure 2c.

Table S7. Datasets used for Prokaryote Frequency-Viscosity analysis (Fig. S5)

Panel	Species	Medium	ΔAIC	n	Source
a	*Brachyspira pilosicoli*	Ficoll	26.7	6	Nakamura, S., Adachi, Y., Goto, T. & Magariyama, Y. (2006) *Biophys J* 90, 3019–3026.
		PVP	28.2	7	
b*	*Escherichia coli*	Ficoll	-2.1	24	Berg, H. & Turner, L. (1979) *Nature* 278, 349–351.
		MC	7.9	8	
c	*Escherichia coli*	Ficoll	1.5	8	Yuan, J., Fahrner, K. A. & Berg, H. C. (2009) *J Mol Biol* 390, 394–400.
		Ficoll	-2.0	6	Chen, X. & Berg, H. C. (2000) *Biophys J* 78, 1036–1041.
d	*Escherichia coli* Chimeric motor	Torque	-2.0	42	Inoue, Y. *et al.* (2008) *J Mol Biol* 376, 1251–1259.
e	*Streptococcus* SM197	Ficoll	26.8	20	Lowe, G., Meister, M. & Berg, H. C. (1987) *Nature* 325, 637–640.

AIC difference calculated as $\Delta AIC = AIC_{power} - AIC_{model}$, such that that support for the power model gives a negative value. Media used to adjust viscosity: Dextran; Ficoll; Polyvinyl pyrrolidone (PVP); Methylcellulose (MC); Carboxymethylcellulose (CMC). Panel letters refer to figure S5, starred panel letters indicate dataset is used in figure 2a.

Table S8. Datasets used for Eukaryote Rate-Temperature analysis (Fig. S7)

Panel	Species (tissue)	ΔAIC	n	Source
a	*Alexandrium minutum*	-2.8	5	Lewis, N. I. *et al.* (2006) *Phycologia* 45, 61–70.
		-2.9	4	
		-2.0	5	
b	*Brachionus plicatilis*	0.9	8	Larsen, P. S., Madsen, C. & Riisgård, H. U. (2008) *Aquat Biol* 4, 47–54.
c	*Chilomonas paramecium*	1.0	5	Lee, J. W. (1954) *Physiol Zool* 275–280.
d	*Ciona intestinalis* (pumping)	14.9	10	Petersen, J. K. & Riisgård, H. U. (2006) *Mar Ecol Prog Ser* 88, 9–17.
		11.1	10	
		10.1	9	
		13.0	10	
e	*Colpidium striatum*	-2.0	12	Beveridge, O. S., Petchey, O. L. & Humphries, S (2010) *J Exp Biol* 213, 4223–4231.
f	*Euglena gracilis*	0.1	6	Lee, J. W. (1954) *Physiol Zool* 275–280.
g	*Fabrea salina*	-1.7	7	Marangoni, R., Batistini, A., Puntoni, S. & Colombetti, G. (1995) *J Photoch Photobio B* 30, 123–127.
h	*Gonyaulax polyedra*	-0.2	8	Hand, W. G., Collard, P. A. & Davenport, D. (1965) *Biol Bull* 128, 90–101.
i	*Gyrodinium sp.*	1.9	13	Hand, W. G., Collard, P. A. & Davenport, D. (1965) *Biol Bull* 128, 90–101.
j	*Halichondria panacea* (pumping)	-4.7	7	Riisgård, H. U., Thomassen, S., Jakobsen, H., Weeks, J. M. & Larsen, P. S. (1993) *Mar Ecol Prog Ser* 96, 177–188.
		-1.5	9	
		1.5	10	
		-0.3	10	
k	*Hiatella arctica (pumping)*	-2.1	6	Ali, R. M. (1970) *Mar Biol* 6, 291–302.

l	*Homo sapiens* (sperm)	-2.0	14	Auger, J., Serres, C. & Feneux, D. (1990) *Cell Motil Cytoskeleton* 16, 22–32.
m	*Mesodinium rubrum*	-1.8	69	Riisgård, H. U. & Larsen, P. S. (2009) *Mar Biol Res* 5, 585–595.
n	*Mya arenaria* (pumping)	-0.3	14	Riisgård, H. U. & Seerup, D. (2003) *Sarsia* 88, 416–428.
o*	*Mytilis edulis* (pumping)	1.9	16	Kittner, C. & Riisgård, H. U. (2005) *Mar Ecol Prog Ser* 305, 147–152.
		-1.2	14	
		1.9	25	Jørgensen, C. B., Larsen, P. S. & Riisgård, H. U. (1990) *Mar Ecol Prog Ser* 64, 89–97.
p		0.5	9	Gray, J. (1923) *Proc Roy Soc Lond B* 95, 6–15.
q	*Ostrea virginica* (pumping)	13.2	10	Galtsoff, P. (1928) *J Gen Physiol* 11, 415–431.
r	*Paramecium caudatum* IF	3.3	12	Fujishima, M., Kawai, M. & Yamamoto, R. (2005) *FEMS Microbiol Lett* 243, 101–105.
s	*Peranema trichophorum*	7.3	14	Shortess, G. S. (1942) *Physiol Zool* 15, 184–195.
t	*Sabella penicillus (pumping)*	-1.7	24	Riisgård, H. U. & Ivarsson, N. M. (1990) *Mar Ecol Prog Ser* 62, 249–257.
u	*Tetrahymena pyriformis*	10.9	16	Connolly, J. G., Brown, I. D., Lee, A. G. & Kerkut, G. A. (1985) *Comp Biochem Phys A* 81, 303–310.

AIC difference calculated as $\Delta AIC = AIC_{Arrhenius} - AIC_{model}$, such that that support for the Arrhenius model gives a negative value. Panel letters refer to figure S7, starred panel letters (and ΔAIC values) indicate dataset is used in figure 4d.

Table S9. Datasets used for Prokaryote Speed-Temperature analysis (Fig. S8)

Panel	Species (tissue)	ΔAIC	n	Source
a	*Chromatium minus*	3.3	8	Mitchell, J. G., Martinez-Alonso, M., Lalucat, J., Esteve, I. & Brown, S. (1991) *J Bacteriol* 173, 997–1003.
b*	*Escherichia coli*	7.9	6	Iwazawa, J., Imae, Y. & Kobayasi, S. (1993) *Biophys J* 64, 925–933.
		-3.3	8	Maeda, K., Imae, Y., Shioi, J. & Oosawa, F. (1976) *J Bacteriol* 127, 1039–1046.
c	*Proteus mirabilis*	-2.6	6	Schneider, W. R. & Doetsch, R. N. (1977) *Appl Environ Microb* 34, 695–700.
d	*Salmonella typhimurium*	-3.7	5	
e	*Spirilium serpens*	-12.9	6	
f	*Steptococococcus* SM197	-1.6	7	Lowe, G., Meister, M. & Berg, H. C. (1987) *Nature*, 325: 637–640.
g	*Sulfolobus acidocaldarius*	-2.8	4	Lewus, P. & Ford, R. M. (1999) *J Bacteriol* 181, 4020–4025.

AIC difference calculated as $\Delta AIC = AIC_{Arrhenius} - AIC_{model}$, such that that support for the Arrhenius model gives a negative value. Panel letters refer to figure S8, starred panel letters indicate dataset is used in figure 4b.

Table S10. Datasets used for Eukaryote Rate-Viscosity analysis (Fig. S9)

Panel	Species (tissue)	Medium	ΔAIC	n	Source
a	*Bos taurus* (sperm)	Glycerol	34.8	50	Rizvi, A. A. *et al.* (2009) *Int Urol Nephrol* 41, 523–530.
b	*Colpidium striatum*	Ficoll	-3.0	18	Beveridge, O. S., Petchey, O. L. & Humphries, S (2010) *J Exp Biol* 213, 4223–4231.
c	*Didinium nasutum*	Ficoll	-3.7	18	Beveridge, O. S., Petchey, O. L. & Humphries, S (2010) *J Exp Biol* 213, 4223–4231.
d	*Mesodinium rubrum*	PVP	18.3	26	Riisgård, H. U. & Larsen, P. S (2009). *Mar Biol Res* 5, 585–595.
e	*Monodelphis domestica* (sperm)	PVP	-3.9	6	Moore, H. D. M. & Taggart, D. A. *Biol Reprod* 52, 947–953 (1995).
f*	*Mytilus edulis* (pumping)	PVP	24.0	7	Riisgård, H. U. & Larsen, P. S. (2007) *Mar Ecol Prog Ser* 343, 141–150.
g	*Ochromonas danica*	MC	7.4	6	Holwill, M. E. J. & Peters, P. D. (1974) *J Cell Biol* 62, 322–328.

AIC difference calculated as $\Delta AIC = AIC_{power} - AIC_{model}$, such that that support for the power model gives a negative value. Media used to adjust viscosity: Dextran; Ficoll; Polyvinyl pyrrolidone (PVP); Methylcellulose (MC); Carboxymethylcellulose (CMC). Panel letters refer to figure S9, starred panel letters indicate dataset is used in figure 4c.

Table S11. Datasets used for Prokaryote Speed-Viscosity analysis (Fig. S10)

Panel	Species (tissue)	Medium	ΔAIC	n	Source
a	*Brachyspira pilosicoli*	PVP	38.7	7	Nakamura, S., Adachi, Y., Goto, T. & Magariyama, Y. (2006) *Biophys J* 90, 3019–3026.
b	*Campylobacter jejuni*	MC	18.7	11	Ferrero, R. & Lee, A. (1988) *J Gen Microbiol* 134, 53–59.
		MC	2.3	6	Shigematsu, M., Umeda, A., Fujimoto, S. & Amako, K. (1998) *J Med Microbiol* 47, 521–526.
c*	*Escherichia coli* AS-1	PVP	3.9	12	Atsumi, T. *et al.* (1996). *J Bacteriol* 178, 5024–5026.
	Escherichia coli	MC	1.1	8	Ferrero, R. & Lee, A. (1988) *J Gen Microbiol* 134, 53–59.
d	*Helicobacter pylori*	MC	4.2	7	Worku, M. L. *et al.* (1999) *Eur J Gastroen Hepat* 11, 1143–1150.
e	*Pseudomonas aeroginosa*	PVP	-1.6	7	Greenberg, E. P. & Canale-Parola, E. (1977) *J Bacteriol* 132, 356–358.
		MC	-2.0	9	Schneider, W. R. & Doetsch, R. N. (1974) *J Bacteriol* 117, 696–701.
		MC	0.0	7	Shigematsu, M., Umeda, A., Fujimoto, S. & Amako, K. (1998) *J Med Microbiol* 47, 521–526.
f	*Rhizobium lupini*	PVP	16.0	8	Götz, R., Limmer, N., Ober, K. & Schmitt, R. (1982) *J Gen Microbiol* 128, 789–798.
g	*Salmonella enteridis*	MC	7.9	7	Ferrero, R. & Lee, A. (1988) *J Gen Microbiol* 134, 53–59.
h	*Salmonella typhimurium*	PVP	-2.0	8	Götz, R., Limmer, N., Ober, K. & Schmitt, R. (1982) *J Gen Microbiol* 128, 789–798.

		MC	4.6	6	Shigematsu, M., Umeda, A., Fujimoto, S. & Amako, K. (1998) *J Med Microbiol* 47, 521–526.
i	*Spirillium serpens*	MC	-2.0	8	Schneider, W. R. & Doetsch, R. N. (1974) *J Bacteriol* 117, 696–701.
j	*Spirillum gracile*	PVP	-1.8	9	Greenberg, E. P. & Canale-Parola, E. (1977) *J Bacteriol* 132, 356–358.
k	*Spirochaeta aurantia*	PVP	21.3	12	Greenberg, E. P. & Canale-Parola, E. (1977) *J Bacteriol* 131, 960–969.
l	*Spirochaeta halophila*	PVP	2.0	7	Greenberg, E. P. & Canale-Parola, E. (1977) *J Bacteriol* 132, 356–358.
		PVP	2.6	8	Greenberg, E. P. & Canale-Parola, E. (1977) *J Bacteriol* 131, 960–969.
m	*Streptococcus* SM197	Ficoll	16.7	14	Lowe, G., Meister, M. & Berg, H. C. (1987) Nature, 325: 637–640.
n	*Thiospirillium jenense*	MC	-2.6	9	Schneider, W. R. & Doetsch, R. N. (1974) *J Bacteriol* 117, 696–701.
o	*Vibrio cholerae*	MC	-2.3	9	Ferrero, R. & Lee, A. (1988) *J Gen Microbiol* 134, 53–59.
		MC	-2.0	6	Shigematsu, M., Umeda, A., Fujimoto, S. & Amako, K. (1998) *J Med Microbiol* 47, 521–526.
p	*Vibrio* YM4	PVP	6.4	13	Atsumi, T. *et al.* (1996). *J Bacteriol* 178, 5024–5026.
q	*Rhizobium meliloti*	PVP	17.9	8	Götz, R., Limmer, N., Ober, K. & Schmitt, R. (1982) *J Gen Microbiol* 128, 789–798.

AIC difference calculated as $\Delta AIC = AIC_{power} - AIC_{model}$, such that that support for the power model gives a negative value. Media used to adjust viscosity: Dextran; Ficoll; Polyvinyl

pyrrolidone (PVP); Methylcellulose (MC); Carboxymethylcellulose (CMC). Panel letters refer to figure S10 starred panel letters indicate dataset is used in figure 4a.